ELSA: Entropy-based Local Indicator of Spatial Association

Babak Naimi[1,2*], Nicholas A.S. Hamm[3], Thomas A. Groen[4], Andrew K. Skidmore[4,5], Albertus G. Toxopeus[4], Sara Alibakhshi[5]

[1] Institute for Biodiversity and Ecosystem Dynamics, University of Amsterdam, Amsterdam, The Netherlands;

[2]Department for Migration and Immuno-ecology, Max Planck Institute for Ornithology, Am Obstberg 1, 78315, Radolfzell, Germany;

[3]School of Geographical Sciences and Geospatial Research Group, Faculty of Science and Engineering, University of Nottingham, Ningbo, China;

[4]Faculty of Geo-Information Science and Earth Observation (ITC), University of Twente, P.O. Box 217, 7500 AE, Enschede, The Netherlands;

[5]Department of Environmental Science, Macquarie University, NSW 2109, Australia

[6]Department of Built Environment, School of Engineering, Aalto University, P.O. Box 14100, 00076 Espoo, Finland

*__Correspondence:__ Babak Naimi, Institute for Biodiversity and Ecosystem Dynamics, University of Amsterdam, Amsterdam, The Netherlands; Email: naimi.b@gmail.com

Naimi, B., N. A. S. Hamm, T. Groen, A. K. Skidmore, B. Toxopeus and S. Alibakhshi (2019) ELSA: Entropy-based local indicator of spatial association, Spatial Statistics, Vol. 29, pp66-88. doi: 10.1016/j.spasta.2018.10.001

Highlights

- ELSA is a new local statistic can be used for both categorical and continuous spatial data.
- ELSA quantifies the degree of local spatial association of a variable at each location.
- Entrogram quantifies global spatial structure and represent as a variogram-like graph.
- ELSA is a non-parametric reliable and robust statistic.
- The R package, elsa, provides the tools for calculation of ELSA and entrogram.

Abstract

Research on spatial data analysis has developed a number of local indicators of spatial association (LISA), which allow exploration of local patterns in spatial data. These include local Moran's I and local Geary's c, as well as G_i and G_i^* that can be used for continuous or interval variables only. Despite numerous situations where qualitative (nominal/categorical) variables are encountered, few attempts have been devoted to the development of methods to explore the local spatial pattern in categorical data. To our knowledge, there is no indicator of local spatial association that can be used for both continuous and categorical data at the same time.

In this paper, we propose a new local indicator of spatial association, called the entropy-based local indicator of spatial association (ELSA), can be used for both categorical and continuous spatial data. ELSA quantifies the degree of spatial association of a variable at each location relative to the same variable at the neighbouring locations. This indicator simultaneously incorporates both spatial and attribute aspects of spatial association into account. The values of ELSA vary between 0 and 1, which denote highest and lowest spatial association, respectively. We compare ELSA to existing statistics such as Local Moran's *I* and test the power and size of the new statistic. We also introduce the "entrogram", a novel approach for exploring the global spatial structure within the entire area (like a variogram). This study showed that the ELSA is consistent and robust, and is therefore suitable for applications in a wide range of disciplines. The ELSA algorithm is made available as an R-package (elsa).

1. Introduction

Spatial analysis is concerned with exploration and identification of associations over geographical space. Such associations quantify the degree to which a value of a variable measured at one location is dependent on the values of the same variable measured at a specific geographic distance from that location (Cliff and Ord 1981; Goodchild 1986). If such dependency exists in a dataset, the variable is said to exhibit spatial autocorrelation (Sokal and Oden 1978). Several statistics have been developed to quantify spatial autocorrelation both globally and locally. Global measures provide a statistic for the entire field under the assumption of spatial stationarity, *i.e.* the mean and covariance do not vary over space. This assumption is often unrealistic. Recent advances have addressed non-stationarity in the mean through spatially varying coefficient modelling (Finley 2011; Gelfand et al. 2003; Hamm et al. 2015a). Heteroskedasticity in the variance can be addressed through a weighting function (Hamm et al. 2012; Lark 2009) and further efforts have been directed at modelling non-stationary covariance functions (Haskard and Lark 2009; Paciorek and Schervish 2006). Models that address non-stationary are often difficult to implement and there is a lack of standard software tools. Further, these models all provide a global measure of autocorrelation. This may be of limited relevance when local areas are of interest.

Research studies on spatial data analysis developed a number of local spatial statistics (Anselin 1995; Boots 2003; Getis and Ord 1992; Ord and Getis 1995). In contrast to global measures, these statistics allow exploration of local patterns in spatial association (Lloyd 2007). They do not rely on the assumption of global stationarity. Anselin (1995) introduced a set of statistics, called local indicators of spatial association (LISA), including local Moran's *I* and local Geary's *c*, that decompose a single global measure into the contribution of each individual location to explore the locations that are major contributors to the global autocorrelation. These statistics can be used to test if local spatial clustering of similar values around the observation is significantly different from the global mean. Getis and Ord (1992) and Ord and Getis (1995) also defined two local statistics, G_i and G_i^*,

67 which are somewhat different from Anselin's LISAs, indicating local clustering of high and low values.
68 These allow detection of pockets of spatial association that may not be evident when using global
69 statistics (Getis and Ord 1992; Ord and Getis 1995). These methods, however, can be used for
70 continuous or interval variables only. Despite numerous situations where qualitative
71 (nominal/categorical) variables are encountered, only a few attempts have been devoted to develop
72 methods to explore the spatial pattern for categorical data. Examples include early works using joint
73 count statistics (Dacey 1968; Dale 2000; Iyer 1949; Moran 1948), extension of the Moran Coefficient
74 to a wide variety of probability models and linking continuous and discrete variables (Griffith 2010),
75 and more recent works including local indicators for categorical data (LICD) by Boots (2003) and
76 symbolic entropy by Ruiz et al. (2010). The purpose of LICD is to identify the nature and spatial
77 extent of local neighbourhoods that are distinctive or unusual compared to *a priori* expectation in
78 binary categorical data (Boots 2003, 2006). To our knowledge, there is no statistic of local spatial
79 association that can be used for both continuous and categorical data.

80 In this paper, we propose a new local indicator of spatial association, called the entropy-based local
81 indicator of spatial association (ELSA), for exploratory analysis and testing the significance of local
82 spatial association of both categorical and continuous spatial data. In doing so, we address the gaps
83 in the research literature highlighted above. Entropy has its root in thermodynamic and information
84 theory. Entropy based approaches have been applied in many disciplines, as a measure of
85 complexity in physics (Shannon and Weaver 1949), as a measure of diversity or structural complexity
86 in ecology (Anand and Orloci 1996; Ricotta and Anand 2006), and as a measure of information
87 content or uncertainty in information theory (Yeung 2008). This concept has also been used by
88 geographers, economists and social scientists to describe spatial phenomena (Batty 1974, 1976;
89 Heikkila and Hu 2006). Recently, some attempts have been conducted to use the concept of entropy
90 as a measure of spatial contiguity for qualitative data (Ruiz et al. 2010), or to detect spatially varying
91 multivariate relationships (Guo 2010). Matilla-García et al. (2011) highlighted the potential role that

92 entropy-based measures might play in detecting spatial structure. They used spatial symbolic
93 entropy for detecting the order of contiguity (spatial lag) of a spatial dependent process (Matilla-
94 García and Marín 2011).

95 Although entropy-based approaches have been used widely for categorical data (e.g. soil type,
96 classified data), there is a challenge in using entropy for exploratory analysis of continuous data. For
97 these data, the probability density function is often unknown, which is necessary to calculate
98 entropy (Guo 2010). A common solution to this problem in most practical applications is to construct
99 a contingency table by binning (discretizing) a continuous variable into a finite number of classes
100 (Guo 2003; Journel and Deutsch 1993), which then are used as categorical data in the entropy
101 measure. This, however, raises two new challenges. Firstly, binning continuous variables causes
102 information loss in data. Secondly, dissimilarity between binned data is not the same as it is in
103 categorical data. For example, when using a categorical land use map in spatial analysis, no
104 difference in the level of dissimilarity between pairs of classes is assumed. If a continuous variable
105 binned into, for example, five categories (C1, …, C5), then C1 is more similar to C2 than to C5. In this
106 paper, we illustrate how ELSA addresses these challenges.

107 The main objectives of our study are: (1) to introduce a new statistic for measuring and testing local
108 spatial association (ELSA) that can be used for both continuous and categorical spatial data; (2) to
109 explore the application of ELSA for calculating local spatial association and comparing this with other
110 indicators; (3) to demonstrate the usability of ELSA to detect global patterns as well, and calculate a
111 variogram-like global spatial structure, named ‘entrogram’. In addition, we developed a new
112 software package, ‘elsa’, in the R environment of statistical computing (R Development Core Team
113 2017) to freely provide the tools required for calculation of the ELSA statistic and the entrogram.

114

115

2. Entropy

In information theory, the concept of complexity is closely related to predictability. It is the amount of information required to achieve an optimal prediction (Boschetti 2008). The entropy measure is also known as the information content. The Shannon entropy has been defined as an average amount of information to eliminate uncertainty, given by a finite number of events:

$$H = -\sum_{k=1}^{m} p_k \log_2 p_k \qquad (5)$$

where H measures the entropy of a system with a finite number of m possible events, and p_k represents the probability of event k. H is at a maximum when all events occur in equal abundance and can be quantified by $\log_2 m$. This measure can be standardized by dividing by $\log_2 m$, providing a measure of relative entropy ranging between 0 and 1. The function is dimensionless and depends only upon the number of events, not upon any other invariant property of the system to which it is applied (Batty 1976).

3. ELSA statistic

The Entropy based Local indicator of Spatial Association, ELSA, extends the above described entropy measure using a term that summarizes the attribute distance between a location and its neighbourhood locations over a given geographical distance.

Assume $\mathrm{x} = (\mathrm{x}_1, \mathrm{x}_2, \ldots, \mathrm{x}_n)'$ are n observations related to a spatial process at locations $\mathrm{u} = (\mathrm{u}_1, \mathrm{u}_2, \ldots, \mathrm{u}_n)'$. Further, denote by $\alpha = (\alpha_1, \alpha_2, \ldots, \alpha_m)$ the set of possible categories that x_i can take. For a categorical variable, it is usually assumed that pairs of categories are equally dissimilar. There are, however, situations where the level of dissimilarity varies for different pairs of categories. For example, ‘dense forest’ and ’sparse forest’ in a land use map are more similar than a pair of either of

137 these two classes and ‘lake’ (for more details, see the Section "ELSA for categorical data"). Likewise,
138 when the values of a continuous variable are binned (discretized) into categories, the level of
139 dissimilarity varies between categories. By ranking the binned values, the difference between rank
140 numbers can be interpreted as the level of dissimilarity. These levels of dissimilarity between
141 categories are taken into account in the calculation of ELSA.

142 ELSA (*E* statistic) at site i is defined as:

$$E_i = E_{ai} \times E_{ci} \tag{6}$$

$$E_{ai} = \frac{\sum_j \omega_{ij} d_{ij}}{\max\{d\} \sum_j \omega_{ij}}, j \neq i$$

$$E_{ci} = -\frac{\sum_{k=1}^{m_\omega} p_k \log_2(p_k)}{\log_2 m_i}, j \neq i$$

$$m_i = \begin{cases} m \text{ if } \sum_j \omega_{ij} > m \\ \sum_j \omega_{ij}, \text{ otherwise} \end{cases}$$

$$d_{ij} = |c_i - c_j|$$

143 where ω_{ij} is a binary weight which specifies whether the site j is within a specified distance (defines
144 the neighbourhood size) from site i. d_{ij} describes the dissimilarity between x_i and x_j, which is
145 calculated as the absolute difference of the ranks assigned to the categories at sites i and j (i.e., c_i
146 and c_j), and $\max\{d\}$ is the maximum possible dissimilarity between any pair of observations in the
147 entire dataset. This is discussed for continuous and categorical variables in the upcoming sections.
148 There are m categories in the entire dataset, $p_k$is the probability of k^{th} category from the m_ω

149 categories within the local distance from site i, and $m_i$is the maximum possible number of
150 categories within the local distance from site i. This means that if the number of observations within
151 the local distance from site i, including site i, is greater than the number of categories in the entire
152 dataset ($\sum_j \omega_{ij} > m$), then m_i is equal to the number of categories, otherwise it is equal to the
153 number of observations ($\sum_j \omega_{ij}$) within the local distance from site i.

154 The first term in the equation 6 (E_{ai}) summarizes the attribute distance (dissimilarity) between site i
155 and the neighbouring sites. This coefficient is bounded between 0 and 1. Low values indicate high
156 similarity of site i to neighbouring sites, and high values indicate low similarity with neighbouring
157 sites.

158 The second term of the E_i statistic (i.e., E_{ci}) is the Shannon entropy (equation 5), normalized by
159 $\log_2(m_i)$. This term ranges between 0 and 1. By normalizing, values are invariant to the number of
160 categories present in a dataset. In other words, datasets with different numbers of categories are
161 comparable. For normalizing, m_i is defined in relation to the global number of categories in the
162 entire dataset. This term quantifies composition or diversity of the categories within the local
163 distance from site i, but it is not sensitive to the level of dissimilarities between pairs of
164 observations.

165 Fig. 1 shows the behaviour of the two terms in ELSA as well as ELSA itself at site i in the centre of a 3
166 x 3 window under five scenarios. When a location is surrounded by similar locations (example a),
167 both the dissimilarity and composition statistics (i.e., E_{ai} and E_{ci}, respectively) would be calculated
168 as 0. The composition in the binary maps in examples b and c, is the same, while the dissimilarity
169 between site i and its neighbour locations in the two maps is different. In example b, the site is
170 surrounded by 8 dissimilar locations to the site, while in the example c, the site is surrounded by 7
171 similar and only one dissimilar locations. Therefore, E_{ai} is at its maximum value in example b, while
172 it is much lower in example c. In the two maps (examples d and e) with three categories, the

dissimilarity is the same for both as the site i is surrounded by 8 dissimilar locations to the site. The composition, however, is different in these two maps.

[Fig. 1]

These five examples show the complementarity of the two terms in the ELSA statistic in different situations. The role of these terms would even be more important if the categories have different levels of dissimilarity (see the upcoming section). It also suggests that either of these terms would be informative on their own for the purpose they are designed for. For instance, if one needs to identify locations with extreme or outlier values, compared to their neighbour locations, the E_{ai} term in ELSA would be the statistic that fulfils the need, while if only the composition (i.e., diversity) of the values within a local neighbourhood is the purpose of the study, the E_{ci} term in ELSA can be used.

3.1. ELSA for categorical data

Categorical variables are typically conceptualized as having no inherent ordering (Ahlqvist and Shortridge 2010), which means that all pairs of categories are equally dissimilar. When using this simplification of class differences and denoting the dissimilarity as d (as in equation 6): $\max(d) = 1$, $d_{ij} = 1$ if $x_i \neq x_j$ and $d_{ij} = 0$ if $x_i = x_j$.

The assumption that all categories are equally dissimilar is often an oversimplification. Several studies have been conducted to estimate a measure of dissimilarity between categories (Romme 1982; Uuemaa et al. 2008). Categories may also be classified into a hierarchical structure. For example, the United Nations Food and Agricultural Organization's (FAO) land cover classification system arranges classes hierarchically (Di Gregorio and Jansen 2009). Such hierarchies may be used to describe the level of dissimilarity. Consider a categorical map with four categories: 'mixed forest' (α_1), 'coniferous forest' (α_2), 'olive groves' (α_3) and 'vineyards' (α_4). These can be grouped under

196 primary categories such that 'mixed forest' and 'coniferous forest' belong to the primary category
197 'forests' (denoted β_1) and 'olive groves' and 'vineyards' belong to 'agricultural areas' (denoted β_2).
198 To calculate E_i for this categorical map, c_i (the rank number for site i) is set to 1 (always), and c_j is
199 set to 1 (if sites i and j are the same), or 2 (if the categories in sites i and j are different, but belong
200 to the same primary category), or 3 (if the categories in sites i and j are different and also belong to
201 different primary categories). Consequently, the level of dissimilarity, d_{ij}, between two different
202 subcategories of the same primary category is set as $d_{ij} = 1$ (e.g., $d(\text{coniferous forest, mixed forest})$
203 $= d(\alpha_1,\alpha_2) = 1)$, and between two different subcategories from different primary categories is set
204 as $d_{ij} = 2$ (e.g., $d(\text{coniferous forest, vineyards}) = d(\alpha_1,\alpha_4) = 2$).

205 To develop this algorithm, we specify the dissimilarity for categorical data as

206 1) If $\alpha_i = \alpha_j$ then $c_i = 1$ & $c_j = 1$therefore $d_{ij} = 0$
207 2) If $(\alpha_i \neq \alpha_j)$ & $(\beta_i = \beta_j)$ then $c_i = 1$ & $c_j = 2$ therefore $d_{ij} = 1$
208 3) If $(\alpha_i \neq \alpha_j)$ & $(\beta_i \neq \beta_j)$ then $c_i = 1$ & $c_j = 3$ therefore $d_{ij} = 2$

209 The level of dissimilarity between pairs of categories can be illustrated in a matrix (Table 1). This
210 makes ELSA flexible enough to handle situations where the level of dissimilarity can be specified for
211 pairs of categories or when categories are hierarchically ordered.

212 **[Table 1]**

213 The above situation can be extended to the case where there are more levels in the hierarchy. The
214 maximum level of dissimilarity is then equal to the degree of hierarchy. In Fig. 2, the level of
215 dissimilarity is presented schematically for a hierarchical system that contains 3 levels.

216 **[Fig. 2]**

217

3.2. ELSA for continuous data

A key step to calculate ELSA for continuous data is that the variable should be first categorized (binned or discretized) into a number of categories; a procedure that may cause information loss. Inspired by Morrison (1972), we propose an estimation of the optimum number of categories that minimizes the information loss. This optimum is the minimum number of categories that is able to reproduce the spatial data statistically (i.e., that minimizes the loss of information through categorization). To find the optimum number of categories, our procedure uses Spearman's rank correlation coefficient, ρ, as a measure of information between the continuous variable and the categorized variable. If the amount of information is not affected through categorizing, the observed correlation should be equal to one. Any loss of information would result in the observed correlation to be less than one. Therefore, the magnitude of the difference $1 - \rho$ provides a measure of information loss (Quester and Dion 1997). The procedure of selecting the optimum number involves the following steps:

1) The categorization procedure starts with a minimum number of categories $m = 2$
2) The procedure assigns a rank number (between 1 and m, where m is the total number of categories) to each category.
3) The ρ coefficient between the continuous values and the assigned ranks is calculated for each iteration.
4) The steps 1 to 3 are repeated, every time by considering one more category (i.e., increasing m), until a convergence threshold (e.g., 0.005) is reached. The convergence is defined as the difference between the ρ coefficients of the current and previous iterations.
5) The one-standard-error rule (James et al. 2013) is applied to select the optimum number of categories. First, the standard error of the ρ coefficients is calculated, and then the optimum number of categories would be the lowest number for which the ρ coefficient is within one standard error of the highest ρ coefficient.

It is assumed that the information loss due to the categorization is not substantial when the optimum number is used. Fig. 3, illustrates an example of using this procedure for a continuous variable.

[Fig. 3]

To calculate ELSA for the continuous map using equation 6, the original continuous data $\mathbf{x}$ are then mapped into the ranked categories: $\boldsymbol{\alpha} = (\alpha_1,\alpha_2,\ldots, \alpha_m)'$ with ranks $c_1,c_2,\ldots, c_m$, where $c_1 = 1$ and $c_m = m$. The maximum level of dissimilarity in the entire map is therefore: $\max(d) = c_m - 1$ and the dissimilarity between the categories at two locations $\mathbf{u}_i$ and $\mathbf{u}_j$ is $d_{ij} = |c_i - c_j|$.

4. Inference for ELSA statistic

In this section we propose a non-parametric bootstrap randomization approach to test the local spatial association against a null distribution. The approach is based on repeated resampling from a distribution, $\widehat{F_0}$, which satisfies the relevant null hypothesis (Davison and Hinkley 1997). Suppose $\alpha = (\alpha_1,\alpha_2,\ldots, \alpha_m)$ are the possible events, outcomes of a spatial process, that n observations $x = (x_1,x_2, \ldots, x_n)'$ can take at locations $u = (u_1,u_2,\ldots, u_n)'$. The null surface can be constructed by rearranging or shuffling the locations (Anselin 1995). Once the null surface $\widehat{F_0}$ is constructed, a Monte Carlo simulation with R runs is used to draw a sample with size n from the null distribution through a bootstrap resampling procedure (sampling with replacement) for each run. The observed ELSA statistic at site i (E_i) can be compared to R independent values of the statistic obtained from the corresponding samples independently simulated under the null hypothesis (i.e., no spatial autocorrelation). If these simulated values at site i are denoted by $E_{1i}^*,\ldots,E_{Ri}^*$, then the probability of accepting the null hypothesis (*P*-value) at site i (P_i) can be approximated by (Davison and Hinkley 1997):

$$P_i = \frac{1 + \#\{E_i \geq E_{ir}^*\}}{R + 1} \quad (7)$$

where $\#\{E_i \geq E_{ir}^*\}$ indicates number of times the observed ELSA at site i is greater than or equal to the ELSA values calculated for the bootstrap samples drawn from the null distribution.

4.1. Size and power of the test

We analysed the size and power of our non-parametric test based on the ELSA statistic to investigate whether the test correctly rejects the null hypothesis only when it should be rejected (Bivand 2009). To do so, we conducted a comprehensive set of data simulations to generate both continuous and categorical variables with various levels of no to high spatial autocorrelation. We used an unconditional simulation to construct regular grids of 50×50 grid cells for each variable. Unconditional simulation is a geostatistical technique that generates a realization of a spatially correlated variable, where the spatial correlation is defined by a variogram (Dungan 1999). The circulant-embedding algorithm (Dietrich and Newsam 1993) implemented in the RandomFields package v. 3.0.44 (Schlather 2009) in the R programming environment, v.3.0.1, was used to conduct the unconditional simulation. The effective variogram range (the maximum geographic separation where two points are expected to be autocorrelated) is determined by the scale parameter, ϕ. The variability is determined by the sill, $C + C_0$, where C is the partial sill and C_0 is the nugget and $\gamma = {C}/{(C + C_0)}$ is the proportion of the variability that has spatial structure. An exponential variogram model with an effective autocorrelation range of $3\phi = 50$ cells and an arbitrary sill of 10 was used for all datasets. We controlled the degree of spatial autocorrelation by changing γ in the variogram models. Five levels of γ = 0, 0.25, 0.5, 0.75, and 1 were used to define the variogram models (Fig. 4), giving a transition from no to high spatial autocorrelation, respectively. To generate the categorical variable, we followed a second step where the continuous spatially autocorrelated variable Y was

used to define a discrete spatial process as follows Ruiz et al. (2010). Let b_{ik} be i^{th} breaking point in discretizing Y into k categories, and defined as:

$$p(Y \leq b_{ik}) = \frac{i}{k} \quad with\ i < k \tag{8}$$

Let $A = \{\alpha_1, \alpha_2, \ldots, \alpha_k\}$ and define the discrete spatial process as:

$$X_{\mathrm{u}} = \begin{cases} \alpha_1 & if\ Y_{\mathrm{u}} \leq b_{1k} \\ \alpha_i & if\ b_{i-1k} \leq Y_{\mathrm{u}} \leq b_{ik} \\ \alpha_k & if\ Y_{\mathrm{u}} \geq b_{k-1k} \end{cases} \tag{9}$$

where X_{u} is the value of discretized Y at location u. For each level of spatial autocorrelation, we generated three sets of categorical variables with k=2, 3, and 4 categories, and a set of continuous variables (Fig. 5).

[Fig. 4]

[Fig. 5]

For each set of data, 999 replicates were simulated and a test with 999 (=R) runs was applied to each replicate at a level of significance $\alpha = 0.05$. We applied the test at the center of the image with different local neighbourhood sizes Ne = 1.5, 3, 5, 10, and 15 cells. We then recorded the number of times that the null hypothesis is rejected (i.e., when $P \leq 0.05$) to quantify the rejection rate. We would expect that the statistic fails to reject the null hypothesis most of the times when the level of spatial autocorrelation is zero (size of the statistic). At the same time, we would expect that it rejects the null hypothesis more frequently (power of the statistic) as the level of autocorrelation goes up (Ruiz et al. 2010).

306 **[Table 2]**

307 The results of the numerical analyses are illustrated in Table 2 for different settings. For the all cases,
308 the power and size of the test showed that the statistic performed reasonably well. The power of
309 the test goes up when the level of spatial autocorrelation increases. The power was slightly higher
310 for the continuous variables compared to the categorical variables. The size was also slightly higher
311 for the continuous variables with smaller neighbourhood sizes, indicating a slightly greater risk for
312 false positive compared to the categorical variables. The results showed that increasing the number
313 of categories in the categorical variables has less effect on the power and size of the statistic. Not
314 surprisingly, there is a loss in the power of the statistic when the neighbourhood size is increased
315 because as the distance is increased, the level of spatial association in decreased. The reason is that
316 as the distance is increased, the level of spatial association is decreased (i.e., increasing the variance
317 in the variogram model).

318

319 ## 5. Application of ELSA to assess local spatial association

320 In this section, we illustrate the use of ELSA by means of several examples using real and synthetic
321 datasets, covering both continuous and categorical variables.

322 *5.1. Experiment with categorical data with the same level of dissimilarity between classes*

323 A land cover map in a raster layer including 2769 grid cells of 1 x 1 km from southern Spain was used
324 for this experiment (Fig. 6-a). The map consists of 6 land cover classes. It is assumed that the level of
325 dissimilarity between pairs of classes is equal. In this experiment, the ELSA was calculated at each
326 cell within a local distance of 5 km (Fig. 6-b). As it was expected, the ELSA statistic becomes 0 for
327 homogenous areas with only one class (mostly at the western part of the area), and when the area

becomes more heterogeneous, the ELSA value becomes higher as it is obvious at the center and eastern parts of the area.

[Fig. 6]

The three specified locations in Fig. 6 (i.e., A, B, and C) and the ELSA values at these locations show how this statistic changes when the landscape changes. By looking at these locations on the land cover map, it can be recognized that the level of heterogeneity changes from low to high from location A to location C.

5.2. Experiment with categorical data with non-equal level of dissimilarity between classes

There are numerous situations where the level of dissimilarity between pairs of classes in a categorical variable is not equal. To show how to deal with these situations, we illustrate two experiments using both synthetic and real data.

-*Synthetic data:* We generated a synthetic categorical raster consisting of 1024 grid cells (32 rows × 32 columns) and four classes (i.e., A1, A2, B1, and B2). The first and second two classes belong to the main categories of A and B, respectively. So, A1 is more similar to A2 than to B1 or B2. The level of dissimilarity between different pairs from the same main category (i.e., A1-A2 or B1-B2) is set to 1, and from different main categories (e.g., A1-B1, A1-B2, etc.) is set to 2 (Fig. 7).

[Fig. 7]

The region is divided into four zones with different combinations of categories. This shows how ELSA changes under these controlled situations. Zone 1 includes only one class (i.e., A1), Zone 2 includes a random distribution of A1 and A2 (i.e., from the same primary category), Zone 3 includes a random distribution of A1 and B1 (i.e., from two different primary categories), and Zone 4 includes random distribution of all four categories.

The maximum level of dissimilarity ($\max\{d\}$) for this experiment is 2. We calculated ELSA at each grid cell using a 3 × 3 window as the local neighbourhood (including diagonal neighbours, i.e., queen's case). We also calculated the mean ELSA for each zone to provide a base for comparison (Fig.8). The results show that the mean ELSA over the two extreme zones are the minimum (Zone 1) and maximum (Zone 4), respectively. The other two zones both follow the same structure (a random distribution of the two classes, but with a different attribute distances). Since Zone 2 consists of two more similar classes than Zone 3, it is expected that the ELSA statistic for the Zone 2 should be lower than Zone 3. This is backed up by the empirical results (Fig. 8-b and Fig. 8-c).

[Fig. 8]

- *Real data:* We used the CORINE [Coordination of Information on the Environment of the European Environmental Agency (EEA 2007)] 2006 land cover map from central Spain including 392336 grid cells of 250 x 250 m. The land cover classes in the map were described using a hierarchical scheme with three levels. The first level indicates the primary land cover class (e.g., agricultural area), which are subdivided to more specific types of land cover classes at the second and third levels (e.g., permanent crops and vineyards at the second and third levels, respectively). A three-digit code is used for each land cover, specifying the class at the three levels from left to right (e.g., 221 and 223

372 are ‘vineyards’ and ‘olive groves’ respectively, i.e., class 1 and 3 specified at the third level,
373 respectively, but both belong to the same classes of ‘agricultural areas’ [class 2] at level 1, and
374 ‘Permanent crops’ [class 2] at level 2). A list of the classes at the three levels for the codes is
375 provided in Table A1 in Appendix A.

376 **[Fig. 9]**

377 The categories were ordered hierarchically at the three levels based on the three-digit codes. The
378 attribute distance (level of dissimilarity) between each pair of categories was calculated based on
379 their position on the hierarchical scheme. The maximum level of dissimilarity is 3 (e.g., between class
380 132 and 211). The dissimilarity between pairs of classes is illustrated in Fig. A1 (the table) & A2 (the
381 hierarchical view) in Appendix A.

382 We calculated ELSA at each grid cell within a local distance of 5 km (Fig. 10). A visual interpretation
383 of the three specified locations on the land cover map (Fig. 9) show that the local association among
384 the three locations is expected to be minimum and maximum at the locations B and C, respectively.
385 The values of the ELSA map at these locations are consistent with the visual interpretation.

386

387 **[Fig. 10]**

388

389 *5.3. Experiment with continuous data*

390 We simulated two synthetic continuous rasters with two levels of no and positive spatial
391 autocorrelation. We used unconditional simulation (see Section 4.1) to construct regular grids of 30
392 $\times 30$ cells for each variable (Fig. 11 & 12). For each raster, we calculated a Moran scatterplot
393 (Anselin 1993), along with global Moran’s I (Moran 1948) to quantify the global spatial

394 autocorrelation and summarize the overall pattern of spatial structure. We calculated ELSA at each
395 cell given a queen contiguity neighbourhood. For comparison, we also quantified other commonly
396 used local indicators of spatial association; G_i^*, local Moran's I and local Geary's c. These statistics
397 were compared pairwised to explore to what extent these measures are related. A Spearman
398 statistic was used to test and estimate a rank-based measure of association test between each pair
399 of statistics.

400 **[Fig. 11]**

401

402 **[Fig. 12]**

403

404 The results from the comparison between different local statistics (Fig. 11 & 12) indicate that when
405 the global spatial autocorrelation is positive, ELSA is only related significantly to local Geary's *c* (ρ =
406 0.675) while the other local indicators are not related either to ELSA or to each other according to
407 the pairwise comparison. When there is no global spatial autocorrelation, ELSA is related
408 significantly to both local Geary's *c* and local Moran's *I*. The former is a positive (ρ = 0.807), and the
409 later is a negative relationship (ρ = -0.563). Local Geary's *c* is also negatively related to local Moran's
410 *I* (ρ = -0.509). The results showed that the Local G^* statistic is not related to any of the other
411 statistics including ELSA. It has been argued that local statistics are sensitive to the existence of
412 global spatial autocorrelation in the dataset (Ord and Getis 2001), that might be the reason to have
413 varying behaviours between the different cases with the positive and no global spatial
414 autocorrelation. For example, we expect a negative relationship between local Moran's *I* and local
415 Geary's *c*, that is shown in the results only when there is no global spatial autocorrelation. The
416 relationship between ELSA and local Geary's *c* is also stronger when there is no autocorrelation

417 compared to the case with positive autocorrelation. The maps of *P*-values based on both ELSA and
418 local Moran's *I* showed that ELSA performed better by resulting in lower *P*-values for most of the
419 grid cells compared to the local Moran's I results, for the case with the positive spatial
420 autocorrelation, that might be because of the sensitivity of the local Moran's *I* to global spatial
421 autocorrelation.

422

423 6. Application of ELSA to assess global spatial structure

424 In this section we explore if global spatial structure can be assessed by employing ELSA into a
425 procedure of generating a sample variogram-like diagram, called 'entrogram'. The idea is that by
426 assessing ELSA with increasing local distances (lags) and putting the averaged values against these
427 distances in a diagram, we can explore spatial structure. The sample variogram is a well-known
428 approach for exploring spatial structure in continuous variables or binary categorical variables (i.e.
429 indicator variogram; Journel 1983). The semantic sample variogram has been developed for
430 multinomial categorical variables (Ahlqvist and Shortridge 2006). If ELSA can be used for this
431 purpose, then the spatial structure for both continuous and categorical variables can be explored
432 with the same technique. The entrogram for lag distance h is calculated as the mean of the ELSA
433 statistics at different sites within the distance equal to the lag size. The entrogram is calculated as
434 follows:

435 $$\mathrm{E}(h) = \frac{\sum_{\mathrm{i}=1}^{\mathrm{n}_h} \mathrm{E_i}(h)}{\mathrm{n}_h} \qquad (7)$$

where $\mathrm{E}(h)$ is the value of the entrogram for distance class h, $\mathrm{E_i}(h)$ is the ELSA statistic at site i within local distance h, n_h is the total number of sites within the distance h for which the ELSA statistic is calculated.

In the following experiments we explored the behaviour of the entrogram for both continuous and categorical data.

6.1. Entrogram for categorical data

We generated five synthetic categorical maps, on a 20 x 20 raster grid, to explore the capability of the entrogram for calculating the spatial structure of categorical maps. The first three maps were binary, one with randomly distributed classes, and the other two with spatially structured classes. These binary maps provide the opportunity to compare the entrogram with the existing method of exploring the spatial structure for a binary categorical variable (i.e. an indicator variogram). The two spatially structured binary maps were constructed using an unconditional simulation with spherical variogram models varying in their autocorrelation range. We used the range of 3 and 8 grid cells to construct the maps with relatively low and high spatial autocorrelation, respectively (Fig. 13).

We quantified both the entrogram, using our developed R package (i.e. elsa), and the indicator variogram using the gstat package v. 1.1-3 (Pebesma 2004) in the R development environment (R Development Core Team 2017). For both, we used a lag size equal to one grid cell and the cutoff values (number of lags) equal to 12 grid cells. The graphs are then visually interpreted and compared (Fig. 12). The results showed that the entrograms indicate the same patterns as the indicator variograms, and therefore can be used to interpret global spatial structure in binary categorical maps.

459 **[Fig. 13]**

460

461 The last two categorical maps were generated with four classes. We assumed that these four classes
462 were equally dissimilar. The classes in the first map were spatially structured, giving a maximum
463 degree of spatial clustering, while in the second map they were distributed randomly. This dataset
464 allowed us to illustrate the capability of the entrogram for exploring the spatial structure of
465 multinomial data. We quantified the entrogram with a lag distance equal to one grid cell and the
466 cutoff value (number of lags) equal to 12 grid cells. The visual interpretation of the graphs (Fig. 14)
467 for the spatially clustered map shows that the mean ELSA value is low within the lower distances and
468 increases when the lag distance increases as would be expected. For the randomly distributed
469 classes, on the other hand, this value remains at the maximum level, showing there is no spatial
470 structure.

471 **[Fig. 14]**

472

473 *6.2. Entrogram for continuous data*

474 We generated five continuous raster maps with different ranges of spatial autocorrelation. We used
475 unconditional simulation to construct regular grids of 200×200 cells for each variable. Two
476 variogram models, a Spherical and a Gaussian model, were used with varying values for the sill ($C +$
477 C_0), nugget (C_0) and scale (ϕ) parameters for different maps. We assigned ϕ different values
478 including ϕ = 10 and ϕ = 30 grid cells giving relative low and high values for the spatial
479 autocorrelation. A total sill, $C + C_0 = 10$, was used for all the datasets, with C_0= 0 for two maps and
480 C_0 = 3 and C_0 = 5 for the other two maps. Additionally, a white-noise surface (ϕ = 0) was simulated,
481 giving a total of five maps with different levels of spatial autocorrelation. We then quantified and

visualized the empirical variogram and entrogram for each surface (Fig. 15). The visual comparisons of the graphs showed that the entrogram describes a global spatial structure similar to the empirical variogram.

[Fig. 15]

7. Discussion

ELSA allows for exploring and testing the local spatial association for both categorical and continuous variables. This provides the opportunity of using one statistic for a study where both types of variables are used, e.g., in species distribution modelling (Naimi and Araújo 2016; Naimi et al. 2014; Naimi et al. 2011), environmental epidemiology (Araujo Navas et al. 2016; Hamm et al. 2015b), and for predicting soil properties (Hengl et al. 2015). The ELSA statistic measures the local spatial associations within the same range (between 0 and 1) for both types of data, making the outputs comparable.

We developed a nonparametric bootstrap test based on the ELSA statistic that is useful to test the hypothesis of independence among spatially distributed quantitative (continuous) and qualitative (categorical) data. Our extensive experiments to demonstrate the size and power of the statistic under a range of conditions suggest the usefulness of the statistic for measuring the local spatial association. In addition, we compared the results of our ELSA test based on a Monte Carlo simulation with the well-known Moran's *I* test. The ELSA test behaved consistent when the global spatial autocorrelation was either positive or zero. The other LISAs showed inconsistent behaviour, i.e., local Moran's *I* and local Geary's *c* only showed the expected negative relationship when the

global autocorrelation was zero. The same holds with the p-values generated by the local Moran's *I* (Fig. 11 & 12). It has been argued that testing the hypothesis of spatial dependence based on LISAs will give incorrect significance levels in the presence of global spatial association (Anselin 1995). This explains why the tests based on local Moran's *I* statistic did not generate the expected p-values when the global spatial autocorrelation was positive. In contrast, our results showed that the ELSA statistic was not sensitive to the presence of the global spatial association that can be considered as an advantage of ELSA over the LISA statistics.

The ELSA calculation for categorical data supports different levels of dissimilarities. This allows evaluation of the dissimilarity between nominal categories in a graded fashion. Several authors in the field of landscape ecology have considered graded differences for measuring landscape patchiness (DeGraaf and Yamasaki 2002; Desrochers et al. 2003). Use of this approach allows transformation from a nominal to an ordered or numerical scale, and provides a foundation for handling attribute distances for categorical data. This is important when quantifying spatial structure for categorical data, since without this aspect all categories are considered equally dissimilar. This approach, however, relies on the subjective evaluation of the class similarity (Ahlqvist and Shortridge 2010), and requires additional data and a guiding theory. Multi-criteria decision making, the analytic hierarchy process, and conjoint analysis are well-known frameworks for evaluating class similarities in categorical maps (Ahlqvist and Shortridge 2010; Schwering 2008). Further studies are needed to characterize and compare these methods, but in this study, we introduced a more general and simple approach to handle class dissimilarities based on a hierarchical scheme of classes. Given additional knowledge about the meaning of class definitions, a more formal evaluation of the categorical dissimilarities can be used to calculate the ELSA statistic for categorical maps.

To measure spatial association, a majority of studies were devoted to the development of statistics for continuous data. In this study, we addressed three of these commonly used statistics and

529 explored how ELSA relates to them. Although all of these statistics have been used widely as
530 measures of local spatial associations, they quantify different properties. Therefore, the appropriate
531 technique for identification of the spatial association should correspond to the nature of the
532 question concerning dependence/independence (Getis and Ord 1996). Our results confirmed these
533 differences and revealed that ELSA is more related to local Geary's *c*. Local Geary's *c* (like in a
534 variogram) is based on differences between pairs of observations. Analogous to variance, entropy is
535 a measure of dissimilarity and diversity, and their equivalence has been explored and discussed in
536 several studies (e.g. Ebrahimi et al. 1999; Lindley 1956).

537 Despite the early specific work in geographical analysis (Batty 1974), entropy has been mainly used
538 in other fields, perhaps mostly in the fields of physics and information theory. The most relevant
539 research (to spatial data) in these disciplines introduced several extensions of the entropy measure
540 that apply to calculating the structural complexity or patterns of two-dimensional dynamical systems
541 (Feldman and Crutchfield 2003; Robinson et al. 2011). In recent years, there were several efforts to
542 develop some entropy-based methods for detecting (global) spatial association and patterns of
543 complexity for univariate data (Matilla-García and Marín 2011; Matilla-García et al. 2012; Pham
544 2010; Ruiz et al. 2010), or as a spatial weighted information measure of global and local spatial
545 association (Karlström and Ceccato 2000), or to discover different forms of local multivariate
546 relationships (Guo 2010). Similar to these methods, ELSA is also based on the entropy measure, but
547 can be considered as a novel approach that offers some unique features, as described in the
548 manuscript.

549 Together with ELSA, this study introduced the entrogram, an approach for exploring the global
550 spatial structure within the entire area (like a variogram). Such explorations are applied in many
551 fields, such as landscape ecology, geography, and soil science. The entrogram uses the ELSA statistic,
552 and therefore, has the advantage over variogram that can be used for different forms of categorical
553 data (e.g., binary-, multinomial-, or hierarchical-classes) as well as continuous data. The indicator

variogram is a known technique to measure the spatial variability of classes in categorical variables. However, it has been argued that the binary treatment of categorical variables in this technique is an unnecessary oversimplification, and that it should be replaced by ordered measures based on semantic similarity evaluations (Ahlqvist and Shortridge 2010). Semantic variograms (Ahlqvist and Shortridge 2006) were developed based on this concern and provide the capability to consider semantic distance between categories in the calculation. We showed that the entrogram is capable of this as well.

We showed that the entrogram can be used as an exploratory tool to characterise global spatial structure. Variograms, however, can also be used for geostatistical modelling and prediction (kriging). Although this study introduced the entrogram as an exploratory tool, future studies may focus on investigating the use of both ELSA and the entrogram for spatial modelling. Moreover, we believe that the ELSA statistic can be adapted for measuring local temporal autocorrelation, local spatio-temporal autocorrelation and multivariate spatial and spatio-temporal autocorrelation. These might be considered as the areas for future research.

Although raster datasets were used in this study to simplify the illustrations, ELSA can be quantified for other types of spatial data (i.e., spatial points and polygons). Our new R package, elsa, offers the functionalities to quantify ELSA, entrogram (as well as variogram and the other LISA statistics) for all the spatial data types. The software is developed using both the R and C programming languages to speed up the computations. All the functionalities in the package are followed by the help pages where their usage and the relevant details, including some examples, are provided.

8. Conclusion

This paper focused on the development of an entropy-based statistic (ELSA) for the quantification of local spatial association. The ELSA statistic presented in this paper showed to be a robust and reliable method for identifying and testing the degree of spatial association. The method provides the advantage of using one statistic for both continuous and categorical data. This makes comparisons between spatial structures of both types of data possible. Another advantage of ELSA, compared to the LISA statistics, is that it is not sensitive to the presence of the global spatial autocorrelation. In addition, this statistic provides the ability to incorporate both spatial and attribute aspects of spatial association into the statistic for both continuous and categorical data. It can be tested for significance, as demonstrated by a power test in this article. By introducing the 'entrogram' we demonstrated that ELSA can also be used to measure global spatial structure of both continuous and categorical data.

References

Ahlqvist, O., & Shortridge, A. (2006). Characterizing Land Cover Structure with Semantic Variograms. In A. Riedl, W. Kainz, & G. Elmes (Eds.), *Progress in Spatial Data Handling* (pp. 401-415): Springer Berlin Heidelberg

Ahlqvist, O., & Shortridge, A. (2010). Spatial and semantic dimensions of landscape heterogeneity. *Landscape Ecology*, *25*, 573-590

Anand, M., & Orloci, L. (1996). Complexity in plant communities: The notion and quantification. *Journal of Theoretical Biology*, *179*, 179-186

Anselin, L. (1993). *The Moran scatterplot as an ESDA tool to assess local instability in spatial association*. Regional Research Institute, West Virginia University Morgantown, WV

Anselin, L. (1995). Local indicators of spatial association—LISA. *Geographical Analysis*, *27*, 93-115

Araujo Navas, A.L., Hamm, N.A.S., Soares Magalhães, R.J., & Stein, A. (2016). Mapping Soil Transmitted Helminths and Schistosomiasis under Uncertainty: A Systematic Review and Critical Appraisal of Evidence. *PLOS Neglected Tropical Diseases*, *10*, e0005208

Batty, M. (1974). Spatial Entropy. *Geographical Analysis*, *6*, 1-31

Batty, M. (1976). Entropy in Spatial Aggregation. *Geographical Analysis*, *8*, 1-21

Bivand, R. (2009). Applying Measures of Spatial Autocorrelation: Computation and Simulation. *Geographical Analysis*, *41*, 375-384

605 Boots, B. (2003). Developing local measures of spatial association for categorical data. *Journal of*
606 *Geographical Systems*, *5*, 139-160
607 Boots, B. (2006). Local configuration measures for categorical spatial data: binary regular lattices.
608 *Journal of Geographical Systems*, *8*, 1-24
609 Boschetti, F. (2008). Mapping the complexity of ecological models. *Ecological Complexity*, *5*, 37-47
610 Cliff, A.D., & Ord, J.K. (1981). *Spatial processes: models and applications*. London: Pion
611 Dacey, M.F. (1968). A review on measures of contiguity for two and k-color maps. In B.J.L. Berry, &
612 D.F. Marble (Eds.), *Spatial analysis: a reader in statistical geography* (pp. 479-495). New Jersey:
613 Prentice-Hall Englewood Cliff
614 Dale, M.R. (2000). *Spatial pattern analysis in plant ecology*. Cambridge university press
615 Davison, A.C., & Hinkley, D.V. (1997). *Bootstrap methods and their application*. Cambridge university
616 press
617 DeGraaf, R.M., & Yamasaki, M. (2002). Effects of edge contrast on redback salamander distribution
618 in even-aged northern hardwoods. *Forest Science*, *48*, 351-363
619 Desrochers, A., Hanski, I.K., & Selonen, V. (2003). Siberian flying squirrel responses to high-and low-
620 contrast forest edges. *Landscape Ecology*, *18*, 543-552
621 Di Gregorio, A., & Jansen, L.J. (2009). *Land cover classification system: LCCS: classification concepts*
622 *and user manual*. Rome: Food and Agriculture Organization of the United Nations
623 Dietrich, C.R., & Newsam, G.N. (1993). A fast and exact method for multidimensional gaussian
624 stochastic simulations. *Water Resources Research*, *29*, 2861-2869
625 Dungan, J. (1999). Conditional Simulation: An alternative to estimation for achieving mapping
626 objectives. In A. Stein, F. Meer, & B. Gorte (Eds.), *Spatial Statistics for Remote Sensing* (pp. 135-152):
627 Springer Netherlands
628 Ebrahimi, N., Maasoumi, E., & Soofi, E.S. (1999). Measuring informativeness of data by entropy and
629 variance. *Advances in Econometrics, Income Distribution and Scientific Methodology* (pp. 61-77):
630 Springer
631 Feldman, D.P., & Crutchfield, J.P. (2003). Structural information in two-dimensional patterns:
632 Entropy convergence and excess entropy. *Physical Review E*, *67*, 051104
633 Finley, A.O. (2011). Comparing spatially-varying coefficients models for analysis of ecological data
634 with non-stationary and anisotropic residual dependence. *Methods in Ecology and Evolution*, *2*, 143-
635 154
636 Gelfand, A.E., Kim, H.-J., Sirmans, C.F., & Banerjee, S. (2003). Spatial Modeling With Spatially Varying
637 Coefficient Processes. *Journal of the American Statistical Association*, *98*, 387-396

638 Getis, A., & Ord, J.K. (1992). The analysis of spatial association by use of distance statistics.
639 *Geographical Analysis*, *24*, 189-206
640 Getis, A., & Ord, J.K. (1996). Local spatial statistics: an overview. In P. Longley, & M. Batty (Eds.),
641 *Spatial analysis: Modelling in a GIS environment* (pp. 261-277). New York: John Wiley
642 Goodchild, M.F. (1986). *Spatial autocorrelation*. Norwich: Geo Books
643 Griffith, D.A. (2010). The Moran coefficient for non-normal data. *Journal of Statistical Planning and*
644 *Inference*, *140*, 2980-2990
645 Guo, D. (2003). Coordinating computational and visual approaches for interactive feature selection
646 and multivariate clustering. *Information Visualization*, *2*, 232-246
647 Guo, D.S. (2010). Local entropy map: a nonparametric approach to detecting spatially varying
648 multivariate relationships. *International Journal of Geographical Information Science*, *24*, 1367-1389
649 Hamm, N.A.S., Atkinson, P.M., & Milton, E.J. (2012). A per-pixel, non-stationary mixed model for
650 empirical line atmospheric correction in remote sensing. *Remote sensing of environment*, *124*, 666-
651 678
652 Hamm, N.A.S., Finley, A.O., Schaap, M., & Stein, A. (2015a). A spatially varying coefficient model for
653 mapping PM10 air quality at the European scale. *Atmospheric Environment*, *102*, 393-405
654 Hamm, N.A.S., Soares Magalhães, R.J., & Clements, A.C.A. (2015b). Earth Observation, Spatial Data
655 Quality, and Neglected Tropical Diseases. *PLOS Neglected Tropical Diseases*, *9*, e0004164
656 Haskard, K.A., & Lark, R.M. (2009). Modelling non-stationary variance of soil properties by tempering
657 an empirical spectrum. *Geoderma*, *153*, 18-28
658 Heikkila, E.J., & Hu, L. (2006). Adjusting spatial-entropy measures for scale and resolution effects.
659 *Environment and Planning B: Planning and Design*, *33*, 845-861
660 Hengl, T., Heuvelink, G.B.M., Kempen, B., Leenaars, J.G.B., Walsh, M.G., Shepherd, K.D., Sila, A.,
661 MacMillan, R.A., Mendes de Jesus, J., Tamene, L., & Tondoh, J.E. (2015). Mapping Soil Properties of
662 Africa at 250 m Resolution: Random Forests Significantly Improve Current Predictions. *PloS one*, *10*,
663 e0125814
664 Iyer, P.K. (1949). The first and second moments of some probability distributions arising from points
665 on a lattice and their application. *Biometrika*, 135-141
666 James, G., Witten, D., Hastie, T., & Tibshirani, R. (2013). *An introduction to statistical learning*.
667 Springer
668 Journel, A.G. (1983). Nonparametric estimation of spatial distributions. *Journal of the International*
669 *Association for Mathematical Geology*, *15*, 445-468
670 Journel, A.G., & Deutsch, C.V. (1993). ENTROPY AND SPATIAL DISORDER. *Mathematical Geology*, *25*,
671 329-355

672 Karlström, A., & Ceccato, V. (2000). A new information theoretical measure of global and local
673 spatial association
674 Lark, R.M. (2009). Kriging a soil variable with a simple nonstationary variance model. *Journal of*
675 *Agricultural, Biological, and Environmental Statistics*, *14*, 301-321
676 Lindley, D.V. (1956). On a Measure of the Information Provided by an Experiment. *The Annals of*
677 *Mathematical Statistics*, *27*, 986-1005
678 Lloyd, C.D. (2007). *Local models for spatial analysis*. CRC/Taylor & Francis London
679 López-Ruiz, R., Mancini, H.L., & Calbet, X. (1995). A statistical measure of complexity. *Physics Letters*
680 *A*, *209*, 321-326
681 Matilla-García, M., & Marín, M.R. (2011). Spatial Symbolic Entropy: A Tool for Detecting the Order of
682 Contiguity. *Geographical Analysis*, *43*, 228-239
683 Matilla-García, M., Ruiz, J.R., & Marín, M.R. (2012). Detecting the order of spatial dependence via
684 symbolic analysis. *International Journal of Geographical Information Science*, *26*, 1015-1029
685 Moran, P.A.P. (1948). The interpretation of statistical maps. *Journal of the Royal Statistical Society*.
686 *Series B (Methodological)*, *10*, 243-251
687 Morrison, D.G. (1972). Regressions with Discrete Dependent Variables: The Effect on R2. *Journal of*
688 *Marketing Research*, *9*, 338-340
689 Naimi, B., & Araújo, M.B. (2016). sdm: a reproducible and extensible R platform for species
690 distribution modelling. *Ecography*, *39*, 368-375
691 Naimi, B., Hamm, N.A.S., Groen, T.A., Skidmore, A.K., & Toxopeus, A.G. (2014). Where is positional
692 uncertainty a problem for species distribution modelling? *Ecography*, *37*, 191-203
693 Naimi, B., Skidmore, A.K., Groen, T.A., & Hamm, N.A.S. (2011). Spatial autocorrelation in predictors
694 reduces the impact of positional uncertainty in occurrence data on species distribution modelling.
695 *Journal of Biogeography*, *38*, 1497-1509
696 Ord, J.K., & Getis, A. (1995). LOCAL SPATIAL AUTOCORRELATION STATISTICS - DISTRIBUTIONAL
697 ISSUES AND AN APPLICATION. *Geographical Analysis*, *27*, 286-306
698 Ord, J.K., & Getis, A. (2001). Testing for local spatial autocorrelation in the presence of global
699 autocorrelation. *Journal of Regional Science*, *41*, 411-432
700 Paciorek, C.J., & Schervish, M.J. (2006). Spatial modelling using a new class of nonstationary
701 covariance functions. *Environmetrics*, *17*, 483-506
702 Pebesma, E.J. (2004). Multivariable geostatistics in S: the gstat package. *Computers & Geosciences*,
703 *30*, 683-691
704 Pham, T.D. (2010). GeoEntropy: A measure of complexity and similarity. *Pattern Recognition*, *43*,
705 887-896

706 Quester, P., & Dion, E. (1997). Scaling Numerical Variables and Information Loss: An Appraisal of
707 Morrison's Work. *MARKETING BULLETIN-DEPARTMENT OF MARKETING MASSEY UNIVERSITY*, *8*, 59-
708 65
709 R Development Core Team (2017). *R: A language and environment for statistical computing*. Vienna,
710 Austria
711 Ricotta, C., & Anand, M. (2006). Spatial complexity of ecological communities: Bridging the gap
712 between probabilistic and non-probabilistic uncertainty measures. *Ecological Modelling*, *197*, 59-66
713 Robinson, M.D., Feldman, D.P., & McKay, S.R. (2011). Local entropy and structure in a two-
714 dimensional frustrated system. *Chaos: An Interdisciplinary Journal of Nonlinear Science*, *21*, 037114-
715 037114-037111
716 Romme, W.H. (1982). Fire and Landscape Diversity in Subalpine Forests of Yellowstone National
717 Park. *Ecological Monographs*, *52*, 199-221
718 Ruiz, M., López, F., & Páez, A. (2010). Testing for spatial association of qualitative data using
719 symbolic dynamics. *Journal of Geographical Systems*, *12*, 281-309
720 Schlather, M. (2009). RandomFields: Simulation and analysis of random fields. In (p. R package
721 version 1.3.41)
722 Schwering, A. (2008). Approaches to Semantic Similarity Measurement for Geo-Spatial Data: A
723 Survey. *Transactions in GIS*, *12*, 5-29
724 Shannon, C.E., & Weaver, W. (1949). The Mathematical Theory of Information. Urbana, IL:
725 University of Illinois Press
726 Sokal, R.R., & Oden, N.L. (1978). Spatial autocorrelation in biology: 1. Methodology. *Biological*
727 *Journal of the Linnean Society*, *10*, 199-228
728 Uuemaa, E., Roosaare, J., Kanal, A., & Mander, Ü. (2008). Spatial correlograms of soil cover as an
729 indicator of landscape heterogeneity. *Ecological Indicators*, *8*, 783-794
730 Yeung, R.W. (2008). *Information theory and network coding*. Springer

731

732

Tables

Table 1 the level of dissimilarity between pairs of categories in an exemplified land use map with four (sub)categories: 'mixed forest' (α_1), 'Coniferous forest' (α_2), 'olive groves' (α_3), 'vineyards' (α_4); the first two belong to the main category of 'Forests' and the last two are related to 'Agricultural areas'

Categories	$\boldsymbol{\alpha_1}$	$\boldsymbol{\alpha_2}$	$\boldsymbol{\alpha_3}$	$\boldsymbol{\alpha_4}$
$\boldsymbol{\alpha_1}$	0	1	2	2
$\boldsymbol{\alpha_2}$		0	2	2
$\boldsymbol{\alpha_3}$			0	1
$\boldsymbol{\alpha_4}$				0

Table 2 Size and power of the ELSA test for continuous, and categorical variables with different degrees of spatial autocorrelation, ranging from no autocorrelation ($\gamma = 0$) to high autocorrelation ($\gamma = 1$); K specifies the number of categories in the categorical variables, and Ne specifies the neighbourhood size for measuring the ELSA statistic

	Ne	$\gamma = 0$	$\gamma = 0.25$	$\gamma = 0.5$	$\gamma = 0.75$	$\gamma = 1$
Continuous	1.5	0.045	0.487	0.882	0.894	0.990
	3	0.048	0.408	0.807	0.916	0.983
	5	0.039	0.398	0.792	0.891	0.977
	10	0.031	0.294	0.734	0.825	0.897
	15	0.012	0.207	0.572	0.650	0.789
K=2	1.5	0.028	0.406	0.787	0.801	0.941
	3	0.017	0.423	0.697	0.787	0.866
	5	0.012	0.412	0.701	0.756	0.840
	10	0.010	0.391	0.639	0.707	0.718
	15	0.002	0.322	0.596	0.650	0.659
K=3	1.5	0.046	0.565	0.705	0.846	0.944
	3	0.005	0.511	0.717	0.827	0.903
	5	0.003	0.495	0.713	0.812	0.892
	10	0.002	0.425	0.601	0.729	0.856
	15	0.000	0.330	0.593	0.698	0.765
K=4	1.5	0.013	0.515	0.741	0.885	0.927
	3	0.011	0.498	0.705	0.822	0.955
	5	0.009	0.413	0.702	0.804	0.926
	10	0.000	0.354	0.619	0.781	0.876
	15	0.000	0.283	0.532	0.773	0.792

Appendix A

Table A1 the CORINE land cover class definitions

CORINE Code	Level 1	Level 2	Level 3
111	Artificial surfaces	Urban fabric	Continuous urban fabric
112	Artificial surfaces	Urban fabric	Discontinuous urban fabric
121	Artificial surfaces	Industrial, commercial and transport	Industrial or commercial
122	Artificial surfaces	Industrial, commercial and transport	Road and rail networks
124	Artificial surfaces	Industrial, commercial and transport	Airports
131	Artificial surfaces	Mine, dump and construction sites	Mineral extraction sites
132	Artificial surfaces	Mine, dump and construction sites	Dump sites
133	Artificial surfaces	Mine, dump and construction sites	Construction sites
141	Artificial surfaces	Artificial, non-agricultural vegetated	Green urban areas
142	Artificial surfaces	Artificial, non-agricultural vegetated	Sport and leisure facilities
211	Agricultural areas	Arable land	Non-irrigated arable land
212	Agricultural areas	Arable land	Permanently irrigated land
221	Agricultural areas	Permanent crops	Vineyards
222	Agricultural areas	Permanent crops	Fruit trees and berry plantations
223	Agricultural areas	Permanent crops	Olive groves
231	Agricultural areas	Pastures	Pastures
241	Agricultural areas	Heterogeneous agricultural areas	Annual crops/permanent crops
242	Agricultural areas	Heterogeneous agricultural areas	Complex cultivation patterns
243	Agricultural areas	Heterogeneous agricultural areas	Land occupied by agriculture
244	Agricultural areas	Heterogeneous agricultural areas	Agro-forestry areas
311	Forest and semi natural	Forests	Broad-leaved forest
312	Forest and semi natural	Forests	Coniferous forest
313	Forest and semi natural	Forests	Mixed forest
321	Forest and semi natural	Scrub and/or herbaceous vegetation	Natural grasslands
323	Forest and semi natural	Scrub and/or herbaceous vegetation	Sclerophyllous vegetation
324	Forest and semi natural	Scrub and/or herbaceous vegetation	Transitional woodland-shrub
331	Forest and semi natural	Open spaces with little/no vegetation	Beaches, dunes, sands
332	Forest and semi natural	Open spaces with little/no vegetation	Bare rocks
333	Forest and semi natural	Open spaces with little/no vegetation	Sparsely vegetated areas
334	Forest and semi natural	Open spaces with little/no vegetation	Burnt areas
411	Wetlands	Inland wetlands	Inland marshes
511	Water bodies	Inland waters	Water courses
512	Water bodies	Inland waters	Water bodies

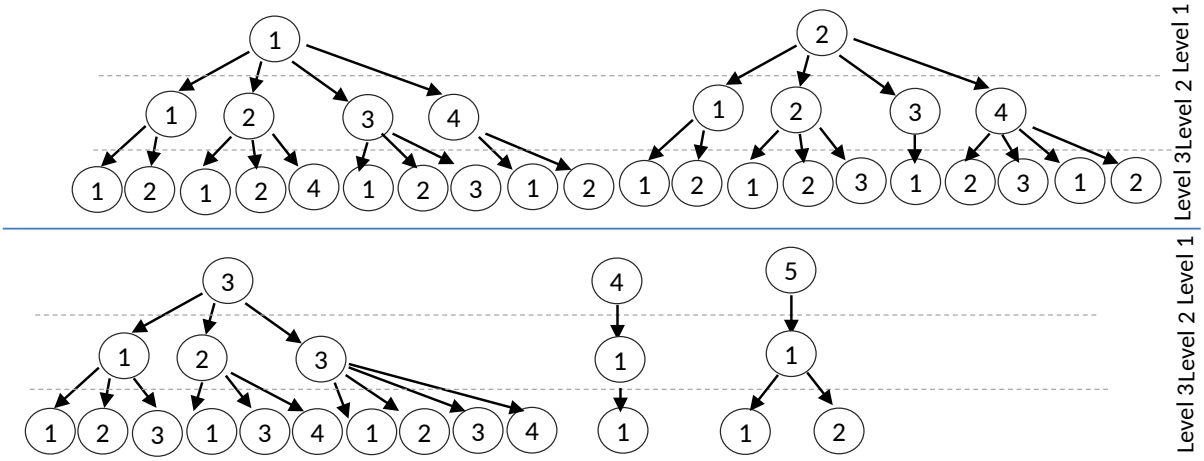

Fig. A1. Hierarchical scheme of different classes in the CORINE land cover map (Fig. 7 in the main text)

774

	111	112	121	122	124	131	132	133	141	142	211	212	221	222	223	231	241	242	243	244	311	312	313	32
111	0	1	2	2	2	2	2	2	2	2	3	3	3	3	3	3	3	3	3	3	3	3	3	3
112		0	2	2	2	2	2	2	2	2	3	3	3	3	3	3	3	3	3	3	3	3	3	3
121			0	1	1	2	2	2	2	2	3	3	3	3	3	3	3	3	3	3	3	3	3	3
122				0	1	2	2	2	2	2	3	3	3	3	3	3	3	3	3	3	3	3	3	3
124					0	2	2	2	2	2	3	3	3	3	3	3	3	3	3	3	3	3	3	3
131						0	1	1	2	2	3	3	3	3	3	3	3	3	3	3	3	3	3	3
132							0	1	2	2	3	3	3	3	3	3	3	3	3	3	3	3	3	3
133								0	2	2	3	3	3	3	3	3	3	3	3	3	3	3	3	3
141									0	1	3	3	3	3	3	3	3	3	3	3	3	3	3	3
142										0	3	3	3	3	3	3	3	3	3	3	3	3	3	3
211											0	1	2	2	2	2	2	2	2	2	3	3	3	3
212												0	2	2	2	2	2	2	2	2	3	3	3	3
221													0	1	1	2	2	2	2	2	3	3	3	3
222														0	1	2	2	2	2	2	3	3	3	3
223															0	2	2	2	2	2	3	3	3	3
231																0	2	2	2	2	3	3	3	3
241																	0	1	1	1	3	3	3	3
242																		0	1	1	3	3	3	3
243																			0	1	3	3	3	3
244																				0	3	3	3	3
311																					0	1	1	2
312																						0	1	2
313																							0	2
321																								0
323																								
324																								
331																								
332																								
333																								
334																								
411																								
511																								
512																								

775 **Fig. A2.** The level of dissimilarity between pairs of classes in the CORINE land cover map

776

Figure Captions

Figure 1. The behaviour of ELSA statistic (E) and its two terms at site *i* (the centre of the window): E_{ai} (first term in ELSA refers to attribute distance or dissimilarity between the site *i* and the its neighbour locations), E_{ci} (second term in ELSA, refers to composition of categories within the local area); (a) is a map with one category, (b, and c) are binary maps, and (d, and e) are maps with three categories.

Figure 2. A hierarchical way of presenting the classes in an exemplified categorical map with 3 levels of categories; the numbers in the boxes indicate d (dissimilarity) of the relevant pairs of classes

Figure 3. A flow diagram showing the procedure of finding the optimum number of categories for categorizing continuous spatial data; (a) an iterative categorization procedure taking different number of categories, starts from 2 categories and continues by considering one more category at each iteration until a convergence threshold (e.g., 0.005) is reached; (b) calculating the ρ correlation coefficient between the continuous values and each categorical variable; the convergence is defined as the difference between the ρ coefficients of the current and previous iterations; (c) taking the standard error of the ρ coefficients is calculated; (d) the optimum number of categories would be the lowest number for which the ρ coefficient is within one standard error of the highest ρ coefficient; (e) the graph representing the ρ coefficients over different iterations and the optimum number of categories (dashed red line); the grey colour represents the standard error of the ρ coefficients

Figure 4. Four variogram models with different nugget effects ranging between 0 and 10, used to simulate the spatial surfaces with different degrees of spatial autocorrelation

Figure 5. One realization (out of 999) of the simulated continuous and categorical maps with various levels of spatial autocorrelation to calculate the power and size of the ELSA statistic; γ is the ratio

between the partial sill to the sill in the variogram model used to simulate the maps (Figure 4) that controls the level of spatial autocorrelation ranging from no autocorrelation (γ=0), and high autocorrelation (γ=1); *K* specifies the number of classes in the categorical maps.

Figure 6. ELSA for a land cover map in the south of Spain; (a) the land cover map including six classes with the same level of dissimilarity between different categories; three cells within their five km neighbourhoods are specified as A, B, C; (b) the ELSA statistic for the land cover map; the values of ELSA for the three cells are represented on top

Figure 7. Synthetic land cover map including four classes which distributions are controlled into four equal zones (a); levels of dissimilarity between pairs of classes in a hierarchical view (b)

Figure 8. The ELSA map (a) and the Mean ELSA statistic in four zones of the region (b); the region is divided into four zones including Z1 (upper-left), Z2 (upper-right), Z3 (lower-right) and Z4 (lower-left); the boxplot (c) represents the distribution of ELSA values at grid cells over different zones

Figure 9. CORINE Land cover map from the central Spain; a three-digit code is used to define each land cover class (a); three randomly selected points around which the circle specifies a 5 km of their neighbors (b)

Figure 10. ELSA map calculated based on the CORINE land cover map in Fig. 7 (a); the ELSA value at the three specified locations (b)

Figure 11. Comparing local indicators of spatial association for a continuous raster map with positive global spatial autocorrelation; the panel contains 12 map/graph/table including the simulated raster map, a Moran scatterplot showing the degree of global spatial autocorrelation, four maps of local Moran's I, local Geary's c, local G_i^*, and ELSA, 2 maps representing the p-values that indicate the

level of significance for local spatial association based on local Moran's I, and ELSA, respectively, and 3 graphs representing the relationship between ELSA on y axis and local Geary's c, local Moran's I, and G_i^* statistics on x axis, and finally a table representing the pairwise spearman correlation coefficients between different local indicators of spatial association; the symbol '***' indicates that the correlation coefficient is significant at the level of 99.9%

Figure 12. Comparing local indicators of spatial association for a continuous raster maps with no global spatial autocorrelation; the different components of the figure are declared in Fig. 11.

Figure 13. Comparing variogram and entrogram for three simulated binary categorical maps with different levels of spatial autocorrelation (ϕ = 0, 3, 8 from left to right); the second and third rows display the corresponding theoretical and empirical variograms, respectively, and the last row displays the entrograms

Figure 14. Two categorical maps including four classes (first row) and their corresponding entrograms (second row)

Figure 15. Comparing variogram and entrogram; the first row displays the 5 simulated continuous fields with different levels of spatial autocorrelation (ϕ = 0, 10, 30, 10, and 10 from left to right), and varying parameterisation in the variogram model, nugget (C_0) and partial sill (C) (as specified in the figure); the second row displays the corresponding variograms and the third row displays the entrograms

Figures

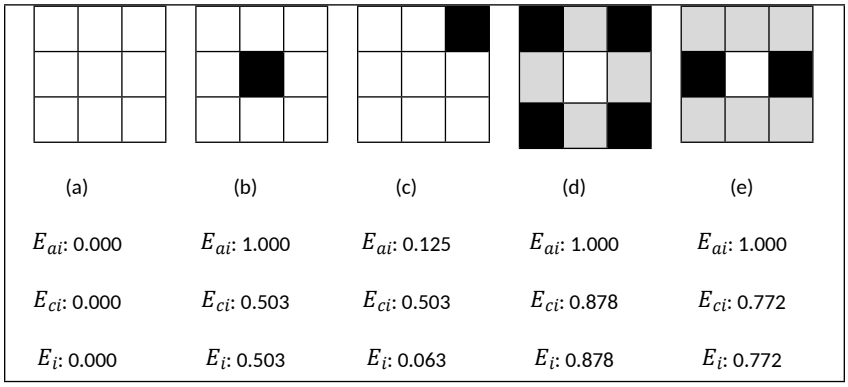

Figure 1

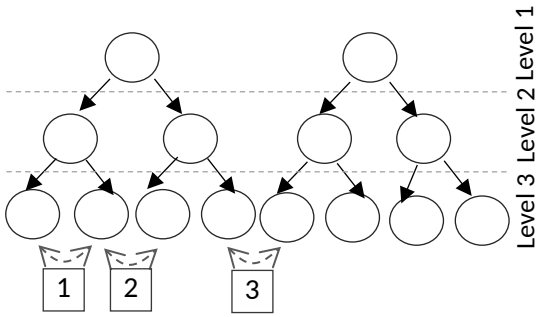

Figure 2.

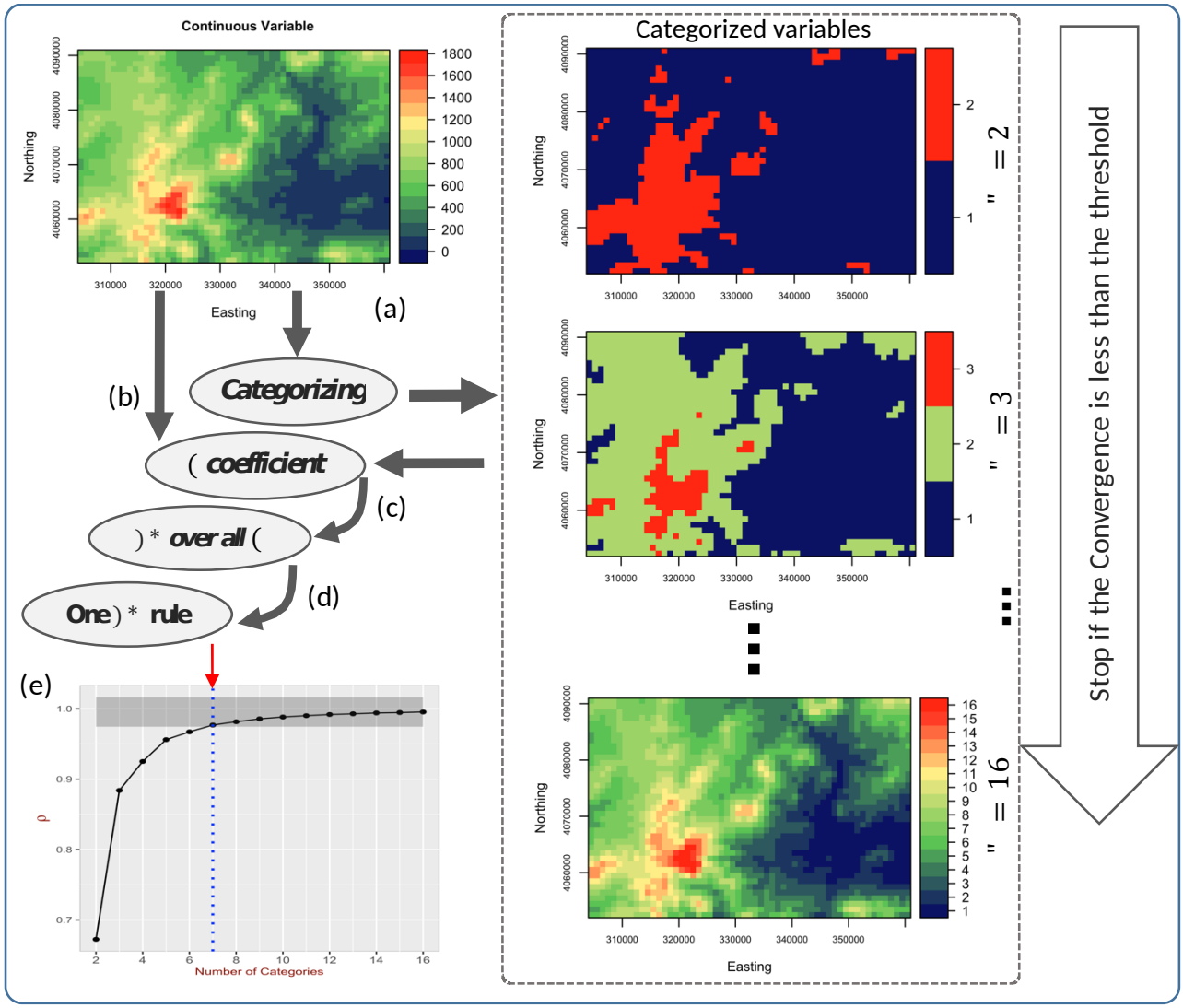
Continuous Variable
Northing
Easting
(a)
(b)
Categorizing
(coefficient
(c)
) * overall (
(d)
One) * rule
(e)
ρ
Number of Categories
Categorized variables
" = 2
" = 3
" = 16
Stop if the Convergence is less than the threshold

Figure 3.

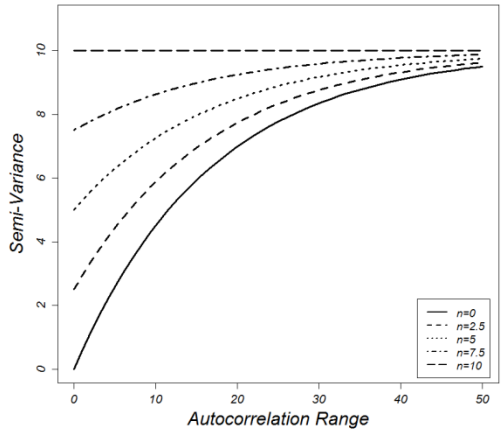
Semi-Variance
0
2
4
6
8
10
0
10
20
30
40
50
Autocorrelation Range
n=0
n=2.5
n=5
n=7.5
n=10

Figure 4.

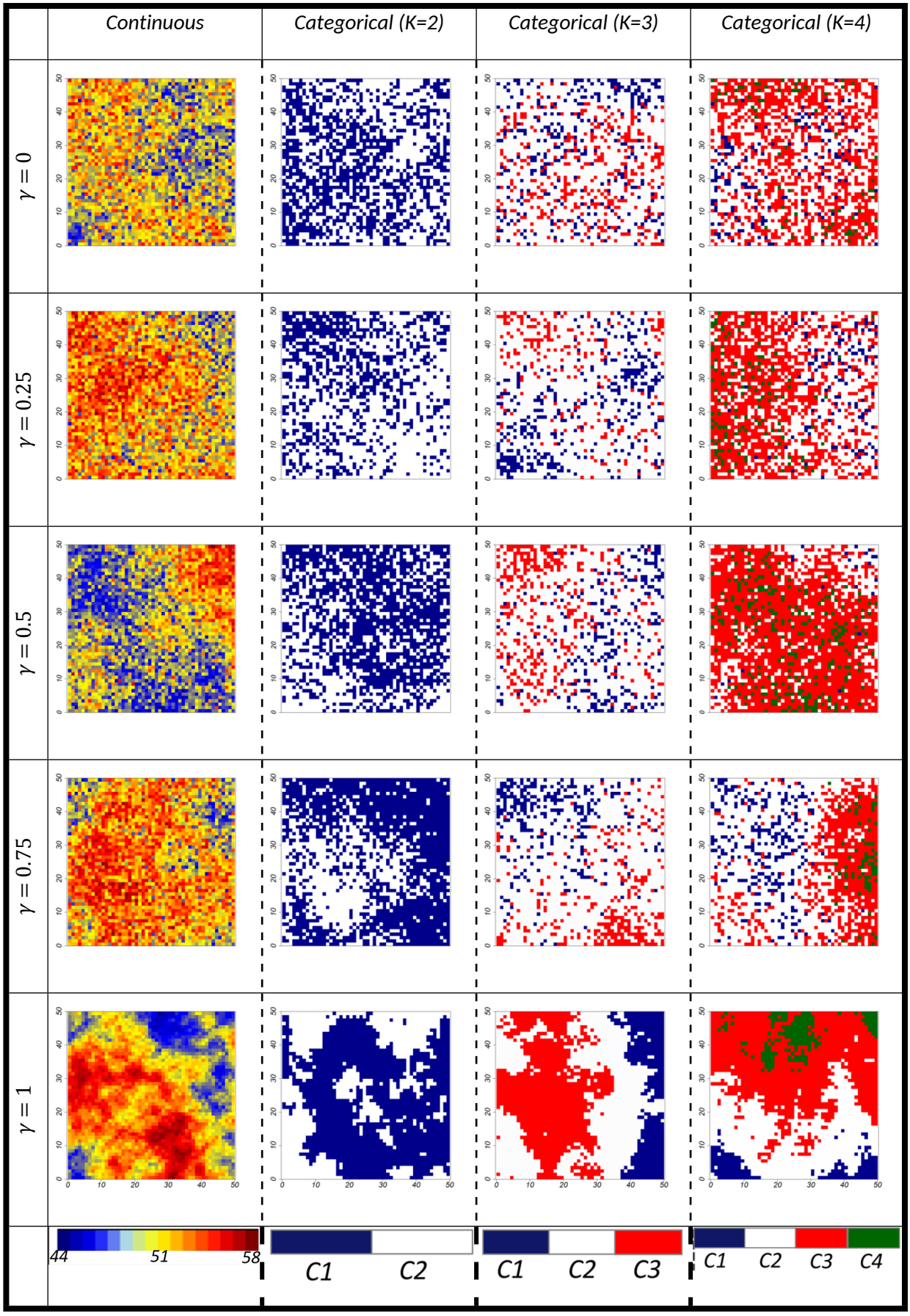
Continuous
Categorical (K=2)
Categorical (K=3)
Categorical (K=4)
$\gamma = 0$
$\gamma = 0.25$
$\gamma = 0.5$
$\gamma = 0.75$
$\gamma = 1$
44
51
58
C1
C2
C1
C2
C3
C1
C2
C3
C4

Figure 5.

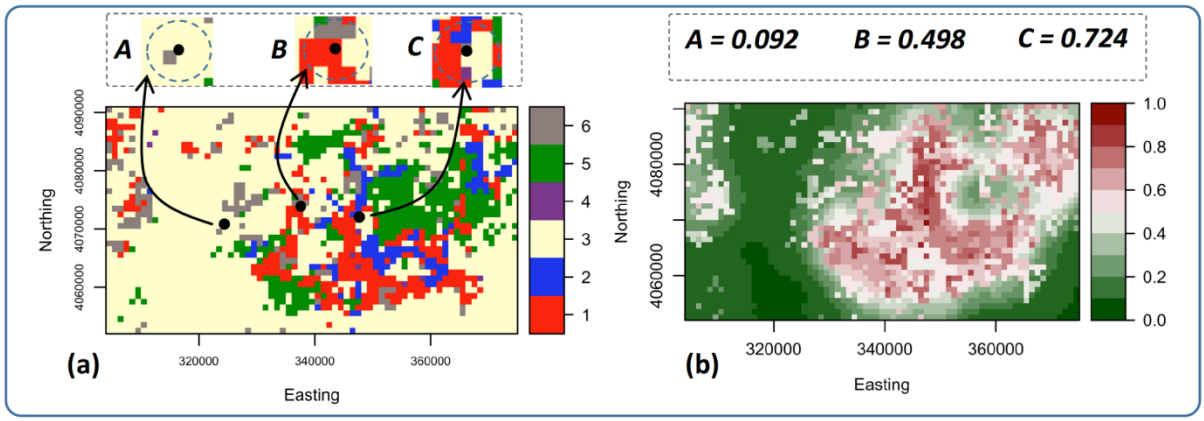
A
B
C
A = 0.092
B = 0.498
C = 0.724
Northing
4060000
4070000
4080000
4090000
320000
340000
360000
Easting
(a)
6
5
4
3
2
1
Northing
4060000
4080000
320000
340000
360000
Easting
(b)
1.0
0.8
0.6
0.4
0.2
0.0

Figure 6

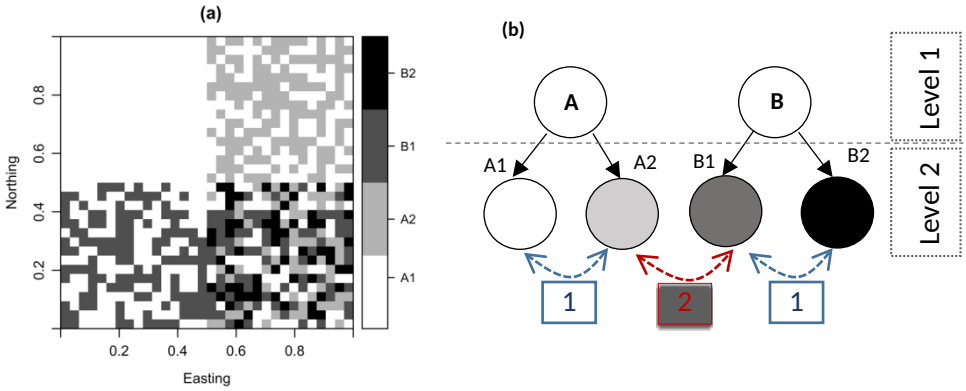
(a)
Northing
0.2
0.4
0.6
0.8
Easting
0.2
0.4
0.6
0.8
B2
B1
A2
A1
(b)
A
B
A1
A2
B1
B2
Level 1
Level 2
1
2
1

Figure 7.

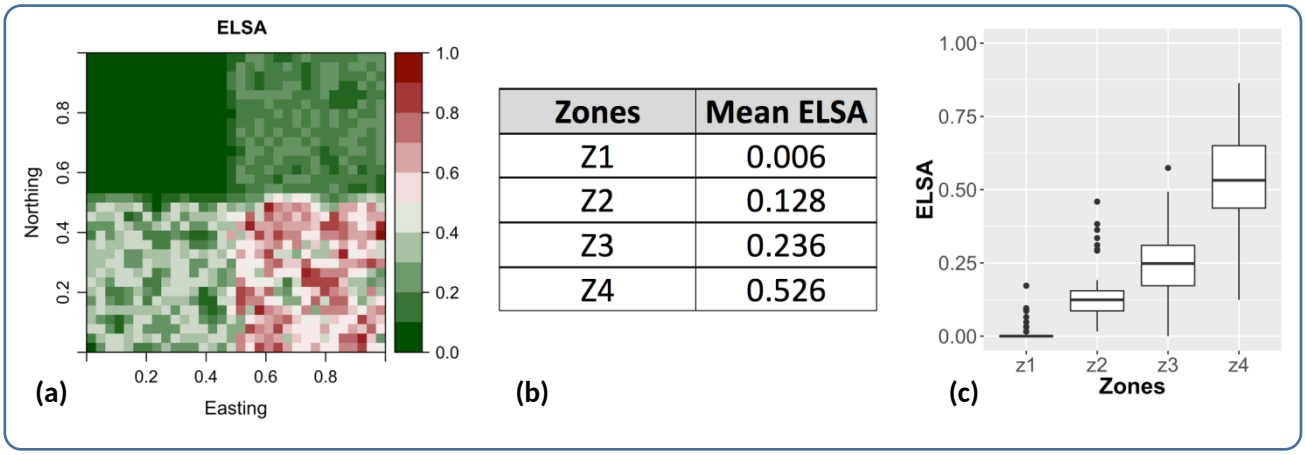

Zones	Mean ELSA
Z1	0.006
Z2	0.128
Z3	0.236
Z4	0.526

Figure 8.

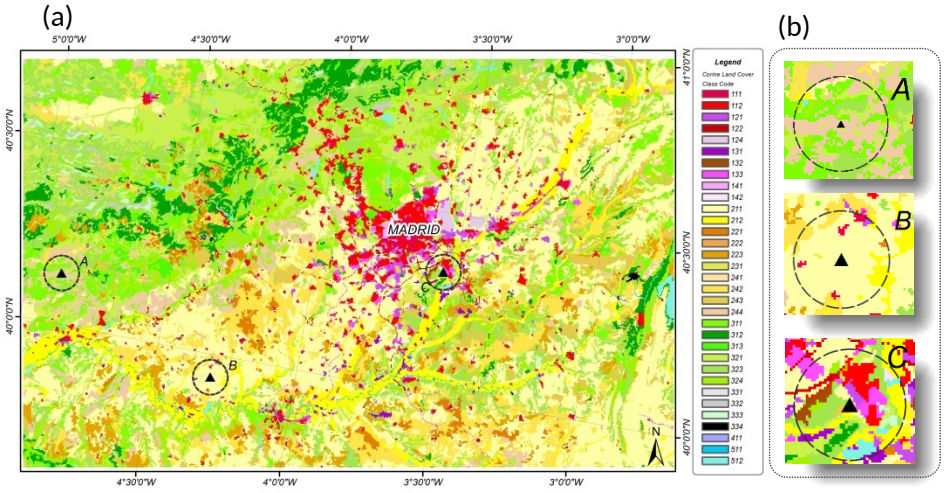
(a)
(b)
MADRID
A
B
C
N
Legend
Corine Land Cover
Class Code
5°0'0"W
4°30'0"W
4°0'0"W
3°30'0"W
3°0'0"W
41°0'0"N
40°30'0"N
40°0'0"N

Figure 9.

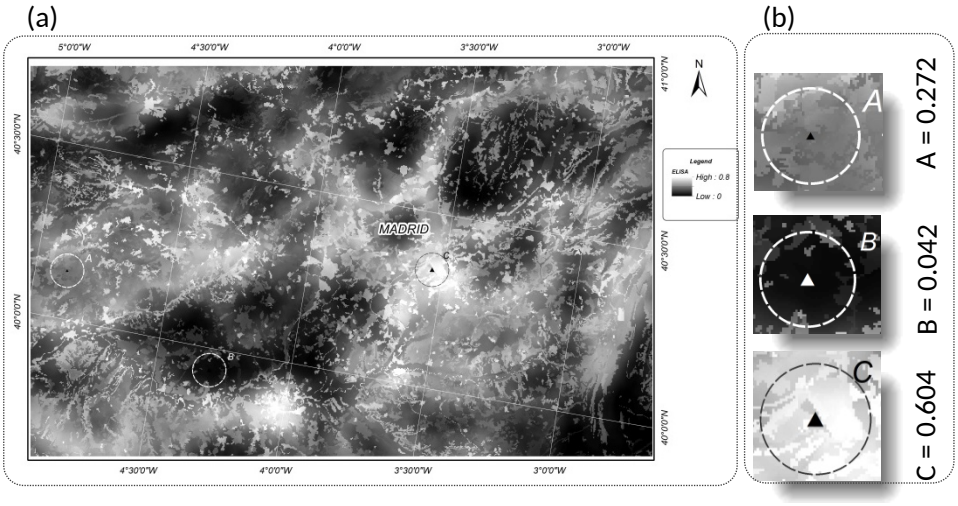
(a)
(b)
5°0'0"W
4°30'0"W
4°0'0"W
3°30'0"W
3°0'0"W
41°0'0"N
40°30'0"N
40°0'0"N
MADRID
A
B
C
N
Legend
ELISA
High : 0.8
Low : 0
A = 0.272
B = 0.042
C = 0.604

Figure 10.

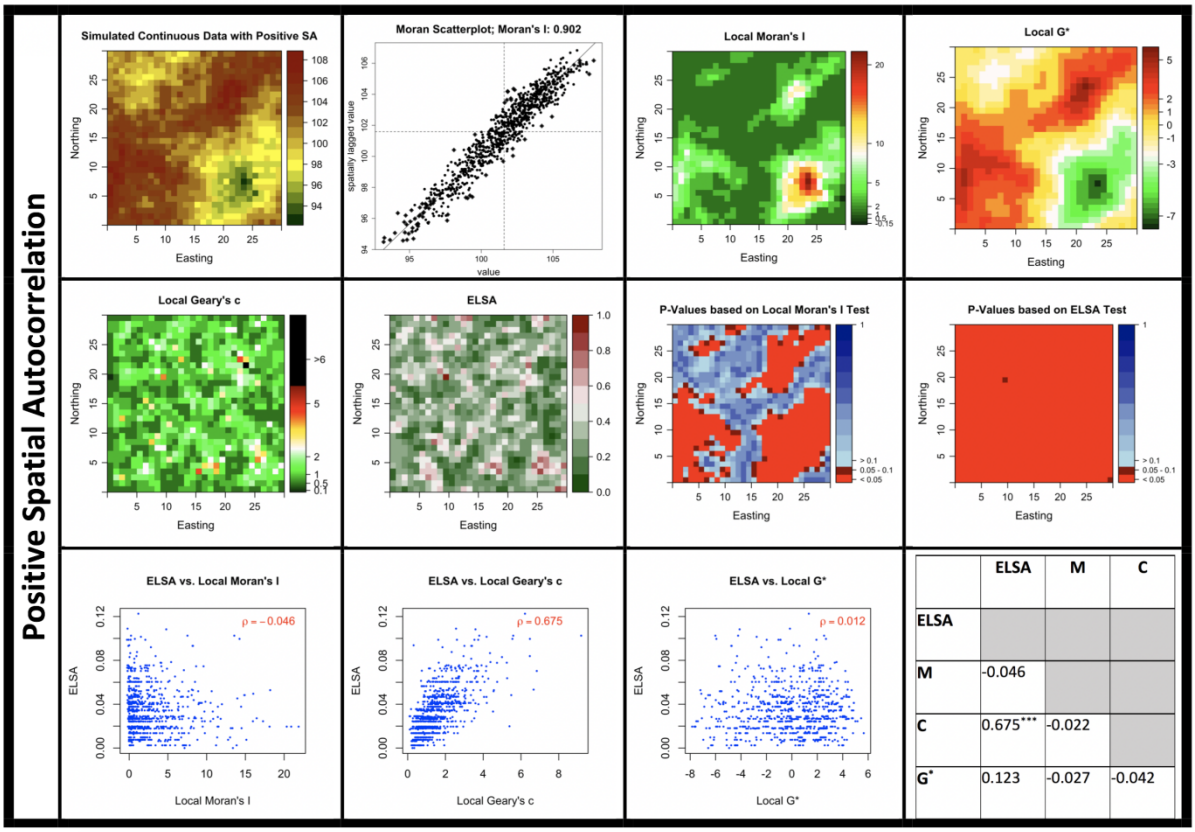

	ELSA	M	C
ELSA			
M	-0.046		
C	0.675***	-0.022	
G*	0.123	-0.027	-0.042

Figure 11

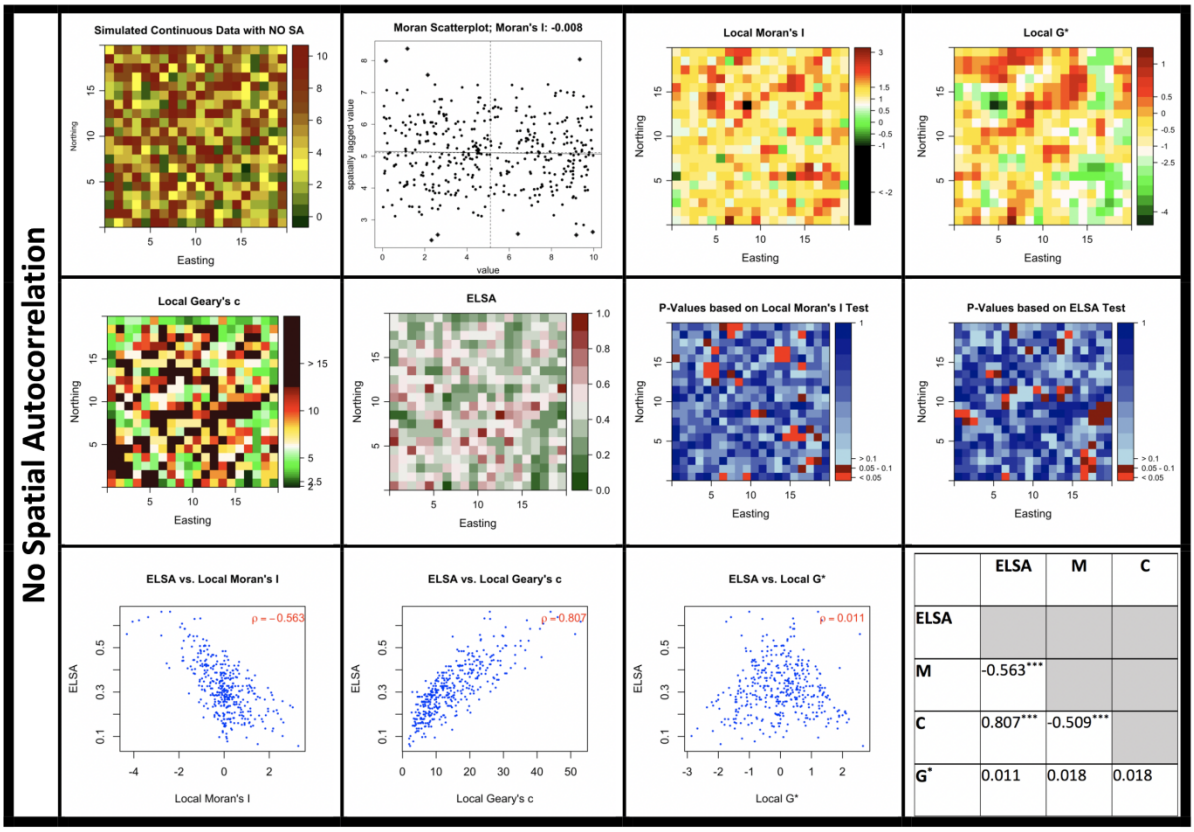

	ELSA	M	C
ELSA			
M	-0.563***		
C	0.807***	-0.509***	
G*	0.011	0.018	0.018

Figure 12.

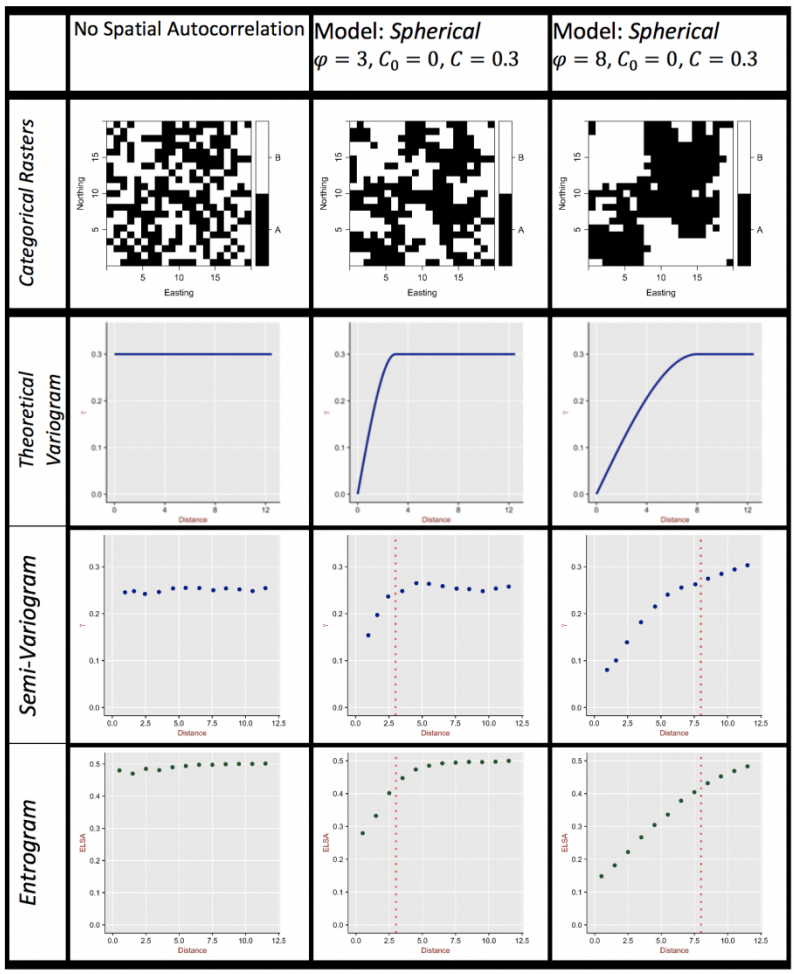
No Spatial Autocorrelation
Model: Spherical
$\varphi = 3, C_0 = 0, C = 0.3$
Model: Spherical
$\varphi = 8, C_0 = 0, C = 0.3$
Categorical Rasters
Theoretical Variogram
Semi-Variogram
Entrogram
Northing
Easting
Distance
ELSA
A
B

Figure 13.

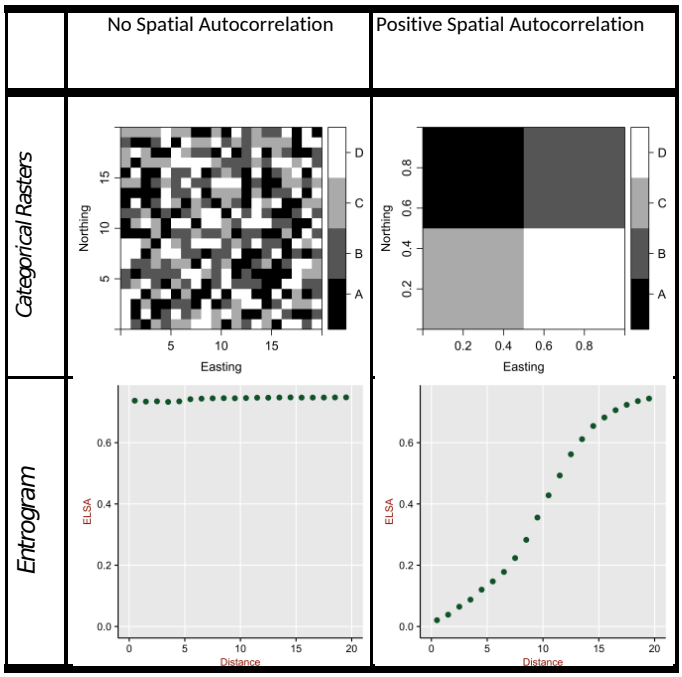
No Spatial Autocorrelation
Positive Spatial Autocorrelation
Categorical Rasters
Entrogram
Northing
Easting
D
C
B
A
ELSA
Distance

Figure 14.

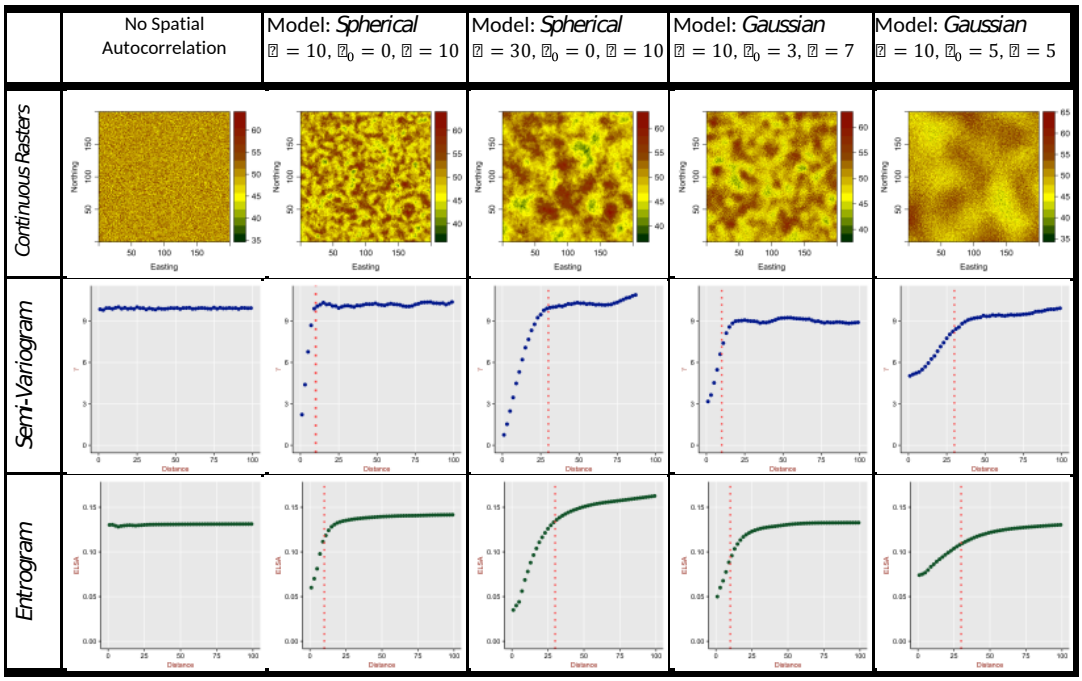
No Spatial Autocorrelation
Model: Spherical
Model: Spherical
Model: Gaussian
Model: Gaussian
Continuous Rasters
Semi-Variogram
Entrogram
Easting
Northing
Distance

Figure 15.